1. Supplementary Figures

a

BRAF Class	BRAF alterations
Class I	$V600^{E/K/R/G/M/V/L/A/D}$
Class II	$Q257^{R}$, $P367^{L/S}$, $E451^{Q}$, $I463^{S}$, $G464^{V/E/R/A}$, $G469^{A/R/V/S}$, $V471^{F}$, $L485^{F/W}$, $N486\_A489^{delinsK}$, $N486\_P490^{del}$, $T488\_P492^{del}$, $K499^{E}$, $L505^{H/F}$, $L525^{R}$, $E586^{K}$, $L597^{R/V/Q/S}$, $E586^{K}$, $T599^{I/R}$, $T599^{dup}$, $V600\_K601^{delinsE}$, $K601^{E/N/Q/T}$
Class III	$F247^{L}$, $D287^{H}$, $G466^{V/E/A/R}$, $S467^{L}$, $G469^{E}$, $K483^{E}$, $R558^{Q}$, $N581^{I/Y/S/T/K}$, $D594^{N/E/G/H/A/Y/V}$, $F595^{L}$, $G596^{R/C/D/V}$, $T599^{A}$

b

BRAF Class	No. of NSCLC patients with BRAF alteration	% of ctDNA positive NSCLC patients	% of BRAF positive NSCLC patients
BRAF Class I Only	845	1.63	34.9
BRAF Class II Only	810	1.56	33.46
BRAF Class III Only	743	1.43	30.69
Multiple Classes	23	0.04	0.95
Total	**2,421**	**4.68**	**100**

c

Frequency of BRAF Class I mutations, NSCLC		
Class I BRAF alterations	# Patients	Percent (%)
V600E	827	97.87
V600K	8	0.95
V600G	4	0.47
V600M	3	0.36
V600R	3	0.36
V600V	3	0.36
V600A	1	0.12
V600L	1	0.12
Total (distinct)	**845**	**100**

d

Frequency of BRAF Class II mutations, NSCLC		
Class II BRAF alterations	# Patients	Percent (%)
G469A	261	32.22
G469V	113	13.95
K601E	106	13.09
G469R	66	8.15
G464V	52	6.42
K601N	33	4.07
L485F	22	2.72
L597Q	21	2.59
Q257R	19	2.35
L597R	17	2.1
E586K	15	1.85
L485W	10	1.23
G464E	8	0.99
G469S	8	0.99
L597V	8	0.99
T599dup	8	0.99
L505F	6	0.74
N486_P490del	6	0.74
V471F	6	0.74
G464A	5	0.62
G464R	4	0.49
L525R	4	0.49
T599I	4	0.49
K499E	3	0.37
K601Q	3	0.37
L505H	3	0.37
T599R	2	0.25
V600_K601delinsE	2	0.25
E451Q	1	0.12
I463S	1	0.12
K601T	1	0.12
Total (distinct)	**810**	**100**

e

Frequency of BRAF Class III mutations, NSCLC		
Class III BRAF alterations	# Patients	Percent (%)
D594N	117	15.75
G466V	111	14.94
D594G	93	12.52
N581S	93	12.52
N581I	63	8.48
G596R	48	6.46
G466A	37	4.98
G466E	34	4.58
G466R	29	3.9
N581Y	27	3.63
G469E	13	1.75
K483E	13	1.75
N581T	12	1.62
D594H	11	1.48
D594E	9	1.21
D594Y	8	1.08
G596C	8	1.08
G596V	6	0.81
F595L	5	0.67
D594A	3	0.4
F247L	3	0.4
G596D	2	0.27
S467L	2	0.27
D287H	1	0.13
D594V	1	0.13
N581K	1	0.13
Total (distinct)	**743**	**100**

Supplementary Figure 1. Frequency of specific BRAF alterations in NSCLC.

a, Classification of BRAF mutations into Class I, II, and III based on their functional and structural

characteristics. Class I includes the common V600 mutations. Class II comprises non-V600 activating mutations in the kinase domain. Class III includes RAS-dependent, kinase-dead or kinase-impaired mutations. **b,** Number and percentage of NSCLC patients (*n* = 2,421) harboring BRAF alterations belonging to Class I only (*n* = 845), Class II only (*n* = 810), Class III only (*n* = 743), or multiple classes (*n* = 23). **c,** Frequency and percentage of patients with specific BRAF Class I alterations, with V600E being the most prevalent (97.87%). **d,** Frequency and percentage of patients with specific BRAF Class II alterations, with G469A (32.22%) and G469V (13.95%) being the most common. **e,** Frequency and percentage of patients with specific BRAF Class III alterations, with D594N (15.75%) and G466V (14.94%) being the most frequent.

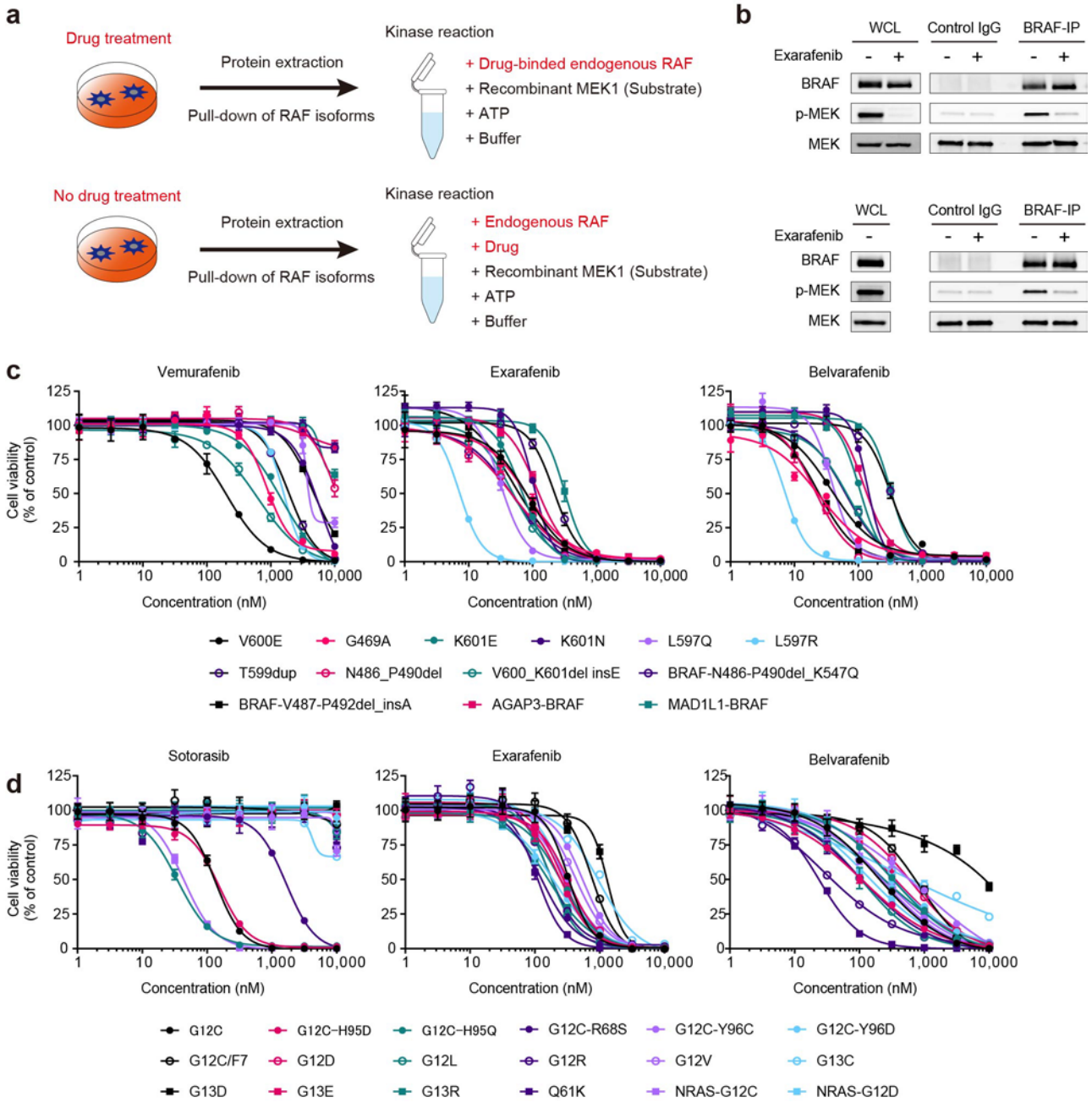

Supplementary Figure 2. Exarafenib inhibits endogenous RAF activity and shows broad efficacy across RAF- and RAS-mutant Ba/F3 models.

a, Schematic representation of the experimental design for assessing the effects of RAF inhibitors on endogenous RAF kinase activity. Two approaches were used: drug administration to cells followed by protein extraction and IP-kinase assay (top), and drug treatment only at the *ex vivo* kinase reaction stage after BRAF-IP (bottom). **b,** Western blot analysis of BRAF kinase activity in the NCI-H2405 cell line treated with exarafenib using the two approaches described in (**a**). **c**, Dose-response curves of vemurafenib,

exarafenib, and belvarafenib in Ba/F3 models expressing various BRAF mutations. Cell viability was assessed after 72 hours of treatment at different drug concentrations. Data are mean ± s.d. A heatmap summarizing the IC50 is shown in Fig. 2d. **d**, Cell viability curves for Fig. 2e. The models include multiple KRAS mutations and some NRAS mutations. Cell viability was measured following 72-hour exposure to varying concentrations of each inhibitor and expressed as a percentage relative to untreated controls. Data are mean ± s.d.

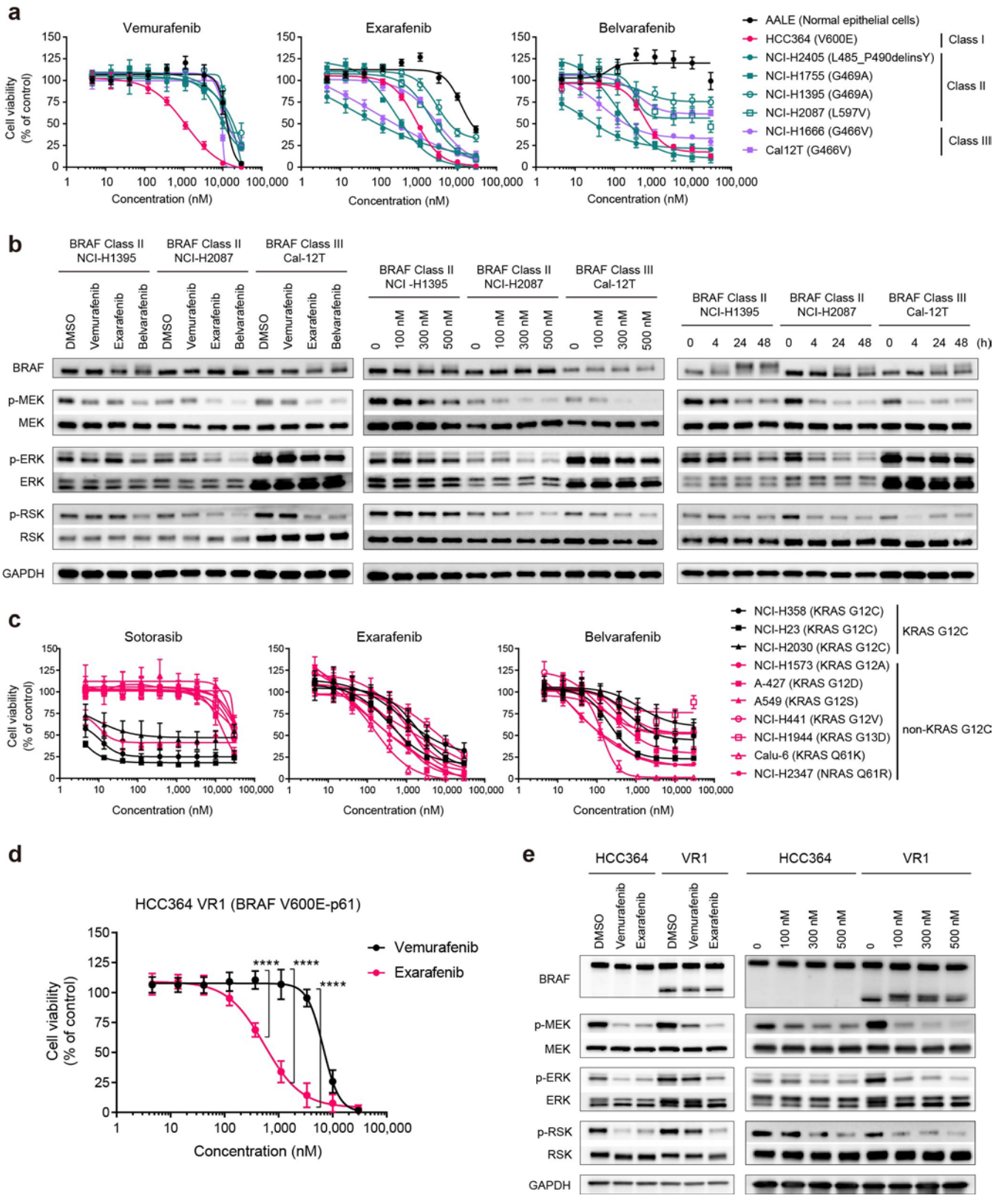
a
Vemurafenib
Exarafenib
Belvarafenib
Cell viability (% of control)
Concentration (nM)
AALE (Normal epithelial cells)
HCC364 (V600E)
NCI-H2405 (L485_P490delinsY)
NCI-H1755 (G469A)
NCI-H1395 (G469A)
NCI-H2087 (L597V)
NCI-H1666 (G466V)
Cal12T (G466V)
Class I
Class II
Class III
b
BRAF Class II NCI-H1395
BRAF Class II NCI-H2087
BRAF Class III Cal-12T
DMSO
Vemurafenib
Exarafenib
Belvarafenib
100 nM
300 nM
500 nM
(h)
BRAF
p-MEK
MEK
p-ERK
ERK
p-RSK
RSK
GAPDH
c
Sotorasib
KRAS G12C
NCI-H358 (KRAS G12C)
NCI-H23 (KRAS G12C)
NCI-H2030 (KRAS G12C)
non-KRAS G12C
NCI-H1573 (KRAS G12A)
A-427 (KRAS G12D)
A549 (KRAS G12S)
NCI-H441 (KRAS G12V)
NCI-H1944 (KRAS G13D)
Calu-6 (KRAS Q61K)
NCI-H2347 (NRAS Q61R)
d
HCC364 VR1 (BRAF V600E-p61)
****
e
HCC364
VR1

Supplementary Figure 3. Exarafenib demonstrates broad-spectrum efficacy against diverse BRAF and KRAS mutations in lung cancer cell lines and overcomes vemurafenib resistance.

a, Dose-response curves showing cell viability of patient-derived lung cancer cell lines harboring BRAF mutations from various functional classes, and the non-cancerous bronchial epithelial cell line AALE, when treated with vemurafenib, exarafenib, or belvarafenib. Data are mean ± s.d. Heatmap depicting the IC50 value is shown in Fig. 3a. **b,** Western blot analysis of MAPK signaling components in lung cancer cell lines with low sensitivity to exarafenib. Left: Various RAF inhibitors tested at a single dose (300 nM) for 4 hours for comparison. Middle: Dose-dependent effects of exarafenib at 4 hours treatment. Right: Time-dependent effects of exarafenib at 300 nM. **c,** Cell viability assay results comparing the effects of sotorasib, exarafenib, and belvarafenib in lung cancer cell lines harboring various KRAS and NRAS mutations. Data are mean ± s.d. **d,** Cell viability assay comparing vemurafenib and exarafenib sensitivity in parental HCC364 and HCC364-VR1 cells. Exarafenib demonstrates higher potency against resistant cells compared to vemurafenib. Data are mean ± s.d. *P*-values at selected points of interest (two-sided Student's *t*-test): 1.3×10^{-9}***, 6.2×10^{-10}***, 1.0×10^{-11}*** (from left to right). *$P < 0.05$, **$P < 0.01$, ***$P < 0.001$, ****$P < 0.0001$. **e,** Western blot analysis of p-MEK, p-ERK and p-RSK in HCC364 and HCC364-VR1 cells treated with vemurafenib or exarafenib. Exarafenib robustly inhibits MAPK signaling in resistant cells.

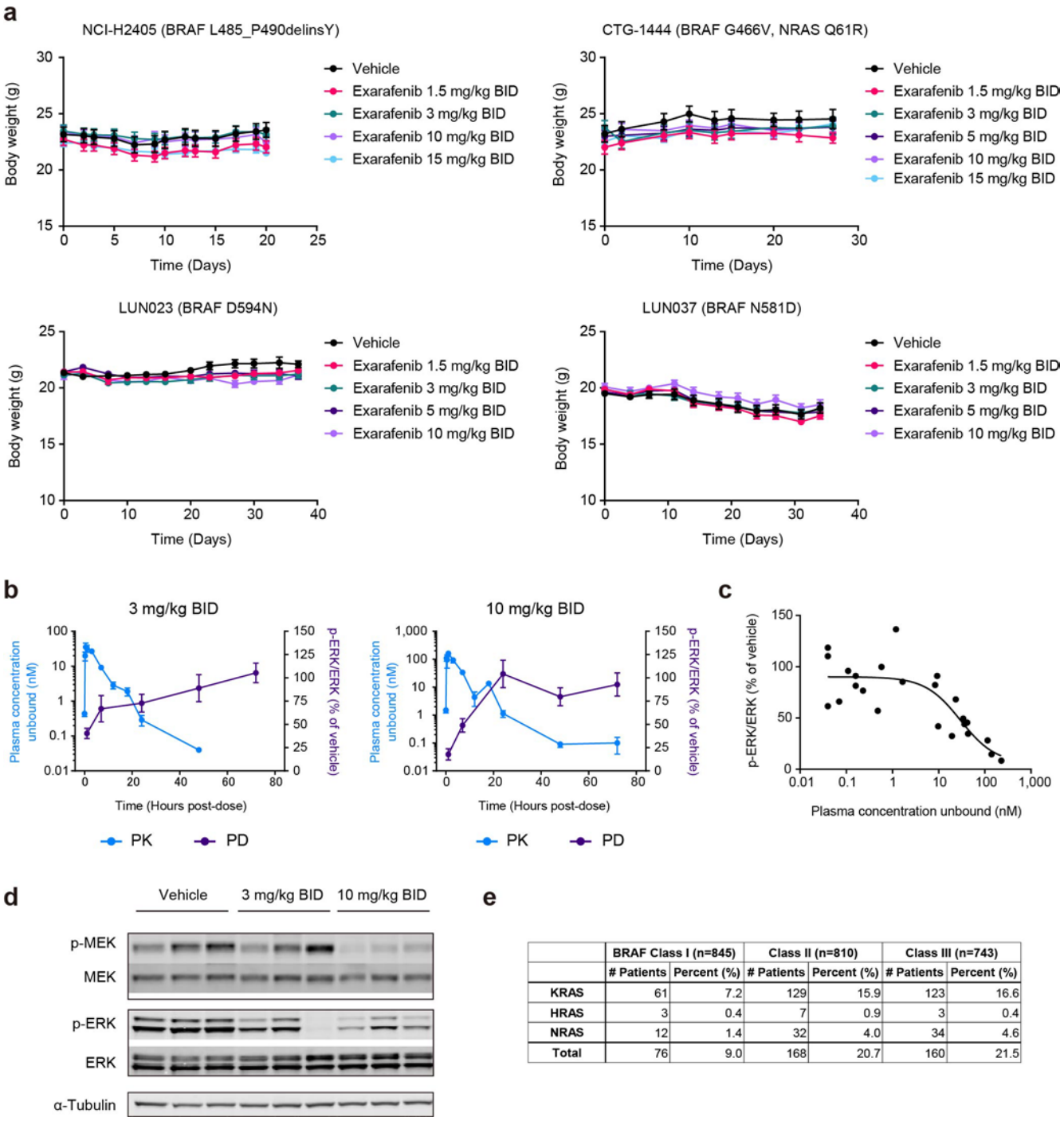

e

	BRAF Class I (n=845)		Class II (n=810)		Class III (n=743)	
	# Patients	Percent (%)	# Patients	Percent (%)	# Patients	Percent (%)
KRAS	61	7.2	129	15.9	123	16.6
HRAS	3	0.4	7	0.9	3	0.4
NRAS	12	1.4	32	4.0	34	4.6
Total	76	9.0	168	20.7	160	21.5

Supplementary Figure 4. Exarafenib demonstrates efficacy in lung cancer models and exhibits dose- and time-dependent pharmacokinetics and pharmacodynamics.

a, *In vivo* tolerability of exarafenib in BRAF-mutant NSCLC xenograft models NCI-H2405 (BRAF L485_P490delinsV), CTG-1444 (BRAF G466V), LUN023 (BRAF D594N), and LUN037 (BRAF N581D). Mice were treated with exarafenib at various dosages twice daily (BID). Body weights were

measured over time. Data represent mean ± s.e.m. (*n* = 9 mice per group). **b,** Pharmacokinetic (PK) and pharmacodynamic (PD) profiles of exarafenib in mice bearing NCI-H2405 xenografts treated with 3 or 10 mg/kg BID for 72 hours. Plasma concentrations confirm linear PK (left y-axis), and p-ERK inhibition in tumor lysates is observed for approximately 24 hours following the final dose (right y-axis). **c,** *In vivo* EC_{50} determination (29.63 nM) based on the relationship between p-ERK inhibition, and plasma concentration of unbound exarafenib in NCI-H2405 xenografts. **d,** Western blot analysis of NCI-H2405 tumor samples treated with vehicle, 3 mg/kg BID, or 10 mg/kg BID doses of exarafenib. Three independent samples from each group were analyzed. The results show dose-dependent inhibition of p-MEK and p-ERK levels. Total MEK (MEK), total ERK (ERK), and α-Tubulin were used as loading controls.

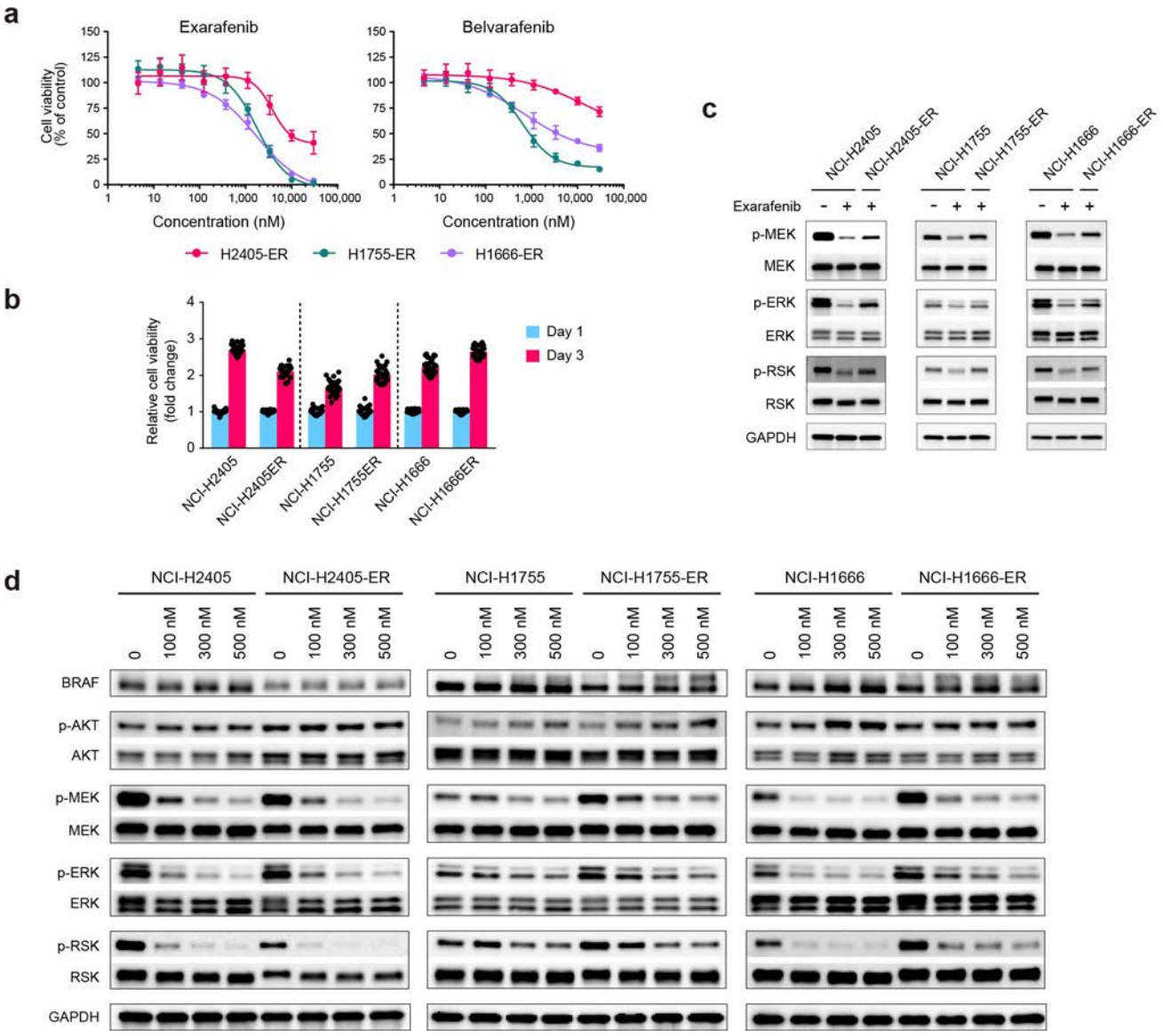

Supplementary Figure 5. Characterization of exarafenib-resistant lung cancer cell lines and their status on MAPK and AKT signaling pathways.

a, Cell viability curves for exarafenib (left) and belvarafenib (right) in exarafenib-resistant cell lines (NCI-H2405-ER, NCI-H1755-ER, and NCI-H1666-ER). Data are mean ± s.d. **b,** Relative cell viability (fold change) of parental cells and their corresponding exarafenib-resistant derivatives. Resistant cells were cultured in the presence of 1μM exarafenib, while parental cells were grown without drug exposure. Measurements were taken on day 1 (blue bars) and day 3 (red bars). Data are presented as fold change relative to day 1. Data are mean ± s.d. The results demonstrate that exarafenib-resistant cell lines maintain proliferation capabilities comparable to their parental counterparts, even under continuous exarafenib exposure. **c,** Analysis of parental and exarafenib-resistant NCI-H2405, NCI-H1755, and NCI-H1666 cell

lines by western blot. Parental cells were treated with either DMSO or 1 μM exarafenib for 4 hours, while resistant cell lines were cultured in 1 μM exarafenib. The levels of p-MEK, p-ERK, and p-RSK were assessed. The resistant cell lines showed sustained levels of p-MEK, p-ERK, and p-RSK compared to their parental counterparts. **d,** Western blot analysis of MAPK and AKT signaling in parental and exarafenib-resistant NCI-H2405, NCI-H1755, and NCI-H1666 cell lines treated with various doses of exarafenib for 4 hours.

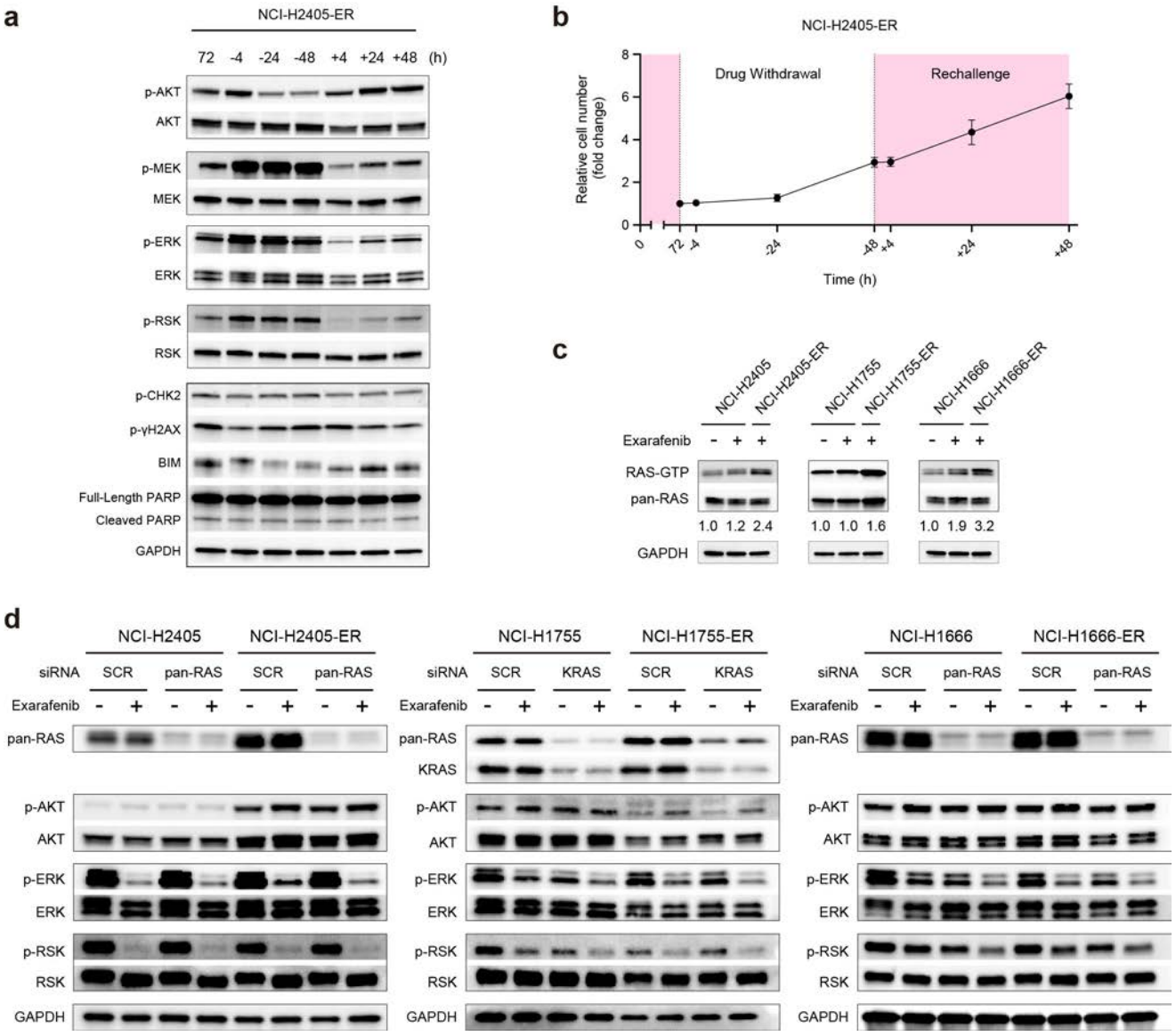

Supplementary Figure 6. RAS-mediated pathway reactivation underlies sustained proliferation in exarafenib-resistant cells

a, Time-course analysis of MAPK pathway components, DNA damage markers, and apoptosis markers in NCI-H2405-ER cells during drug withdrawal and re-challenge. Cells were initially maintained under exarafenib treatment for 72 hours, then switched to drug-free medium (negative timepoints) followed by exarafenib re-treatment (positive timepoints). **b,** Cell number fold change over time for exarafenib-resistant NCI-H2405-ER cells. Cells were initially grown in the presence of exarafenib, then subjected to drug withdrawal (white area), followed by drug re-challenge (red shaded area). Data points represent relative cell number normalized to the 72h time point (set as 1-fold). Data shown as mean ± SD. **c,** RAS-RBD assay assessing RAS activation (RAS-GTP) in parental and resistant cells. Parental cells were treated

with either DMSO or 1 μM exarafenib for 4 hours, while resistant cell lines were cultured in 1 μM exarafenib. **d,** Western blot analysis of RAS knockdown effects on MAPK and AKT signaling in parental and resistant lines. Cells were treated with either DMSO or 500 nM exarafenib for 4 hours.

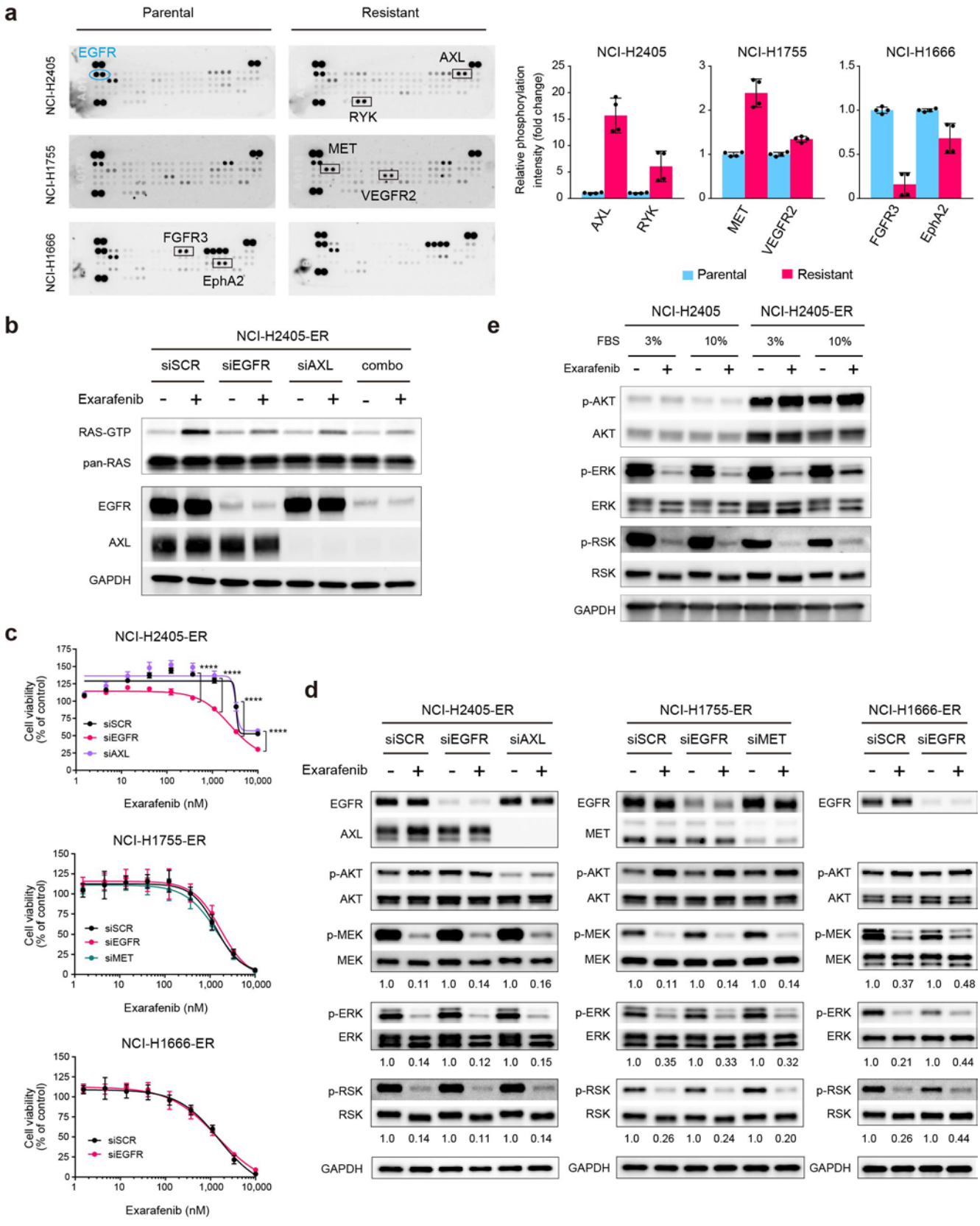
a
Parental
Resistant
NCI-H2405
NCI-H1755
NCI-H1666
EGFR
AXL
RYK
MET
VEGFR2
FGFR3
EphA2
NCI-H2405
NCI-H1755
NCI-H1666
Relative phosphorylation intensity (fold change)
AXL
RYK
MET
VEGFR2
FGFR3
EphA2
Parental
Resistant
b
NCI-H2405-ER
siSCR
siEGFR
siAXL
combo
Exarafenib
RAS-GTP
pan-RAS
EGFR
AXL
GAPDH
e
NCI-H2405
NCI-H2405-ER
FBS
3%
10%
3%
10%
Exarafenib
p-AKT
AKT
p-ERK
ERK
p-RSK
RSK
GAPDH
c
NCI-H2405-ER
Cell viability (% of control)
siSCR
siEGFR
siAXL
Exarafenib (nM)
NCI-H1755-ER
siSCR
siEGFR
siMET
Exarafenib (nM)
NCI-H1666-ER
siSCR
siEGFR
Exarafenib (nM)
d
NCI-H2405-ER
siSCR
siEGFR
siAXL
Exarafenib
EGFR
AXL
p-AKT
AKT
p-MEK
MEK
1.0 0.11 1.0 0.14 1.0 0.16
p-ERK
ERK
1.0 0.14 1.0 0.12 1.0 0.15
p-RSK
RSK
1.0 0.14 1.0 0.11 1.0 0.14
GAPDH
NCI-H1755-ER
siSCR
siEGFR
siMET
EGFR
MET
p-AKT
AKT
p-MEK
MEK
1.0 0.11 1.0 0.14 1.0 0.14
p-ERK
ERK
1.0 0.35 1.0 0.33 1.0 0.32
p-RSK
RSK
1.0 0.26 1.0 0.24 1.0 0.20
GAPDH
NCI-H1666-ER
siSCR
siEGFR
EGFR
p-AKT
AKT
p-MEK
MEK
1.0 0.37 1.0 0.48
p-ERK
ERK
1.0 0.21 1.0 0.44
p-RSK
RSK
1.0 0.26 1.0 0.44
GAPDH

Supplementary Figure 7. RTK profiles and effects of RTK knockdown in exarafenib-resistant lung cancer cell lines.

a, Phospho-RTK array comparing parental and resistant cell lines (left). Black boxes highlight the most significantly changed RTKs in each resistant cell line. The intensity of phosphorylation was quantified and shown as bar graphs (right). Each intensity was normalized using positive controls. **b,** Western blot analysis of RAS activation in NCI-H2405-ER resistant cells following individual and combined RTK knockdown. Cells were transfected with scrambled control (siSCR), siEGFR, siAXL, or combination of both and treated with exarafenib (+) or vehicle (-). **c,** Cell viability curves for exarafenib in NCI-H2405-ER cells transfected with siRNA targeting SCR, EGFR, or AXL (left), NCI-H1755-ER cells transfected with siRNA targeting SCR, EGFR, or MET (middle), and NCI-H1666-ER cells transfected with siRNA targeting SCR or EGFR (right). Data are mean ± s.d. *P*-values at selected points of interest (two-sided Student's *t*-test): 9.72×10^{-13}****, 1.23×10^{-16}****, 8.25×10^{-16}****, 1.29×10^{-18}**** (from left to right). *P < 0.05, **P < 0.01, ***P < 0.001, ****P < 0.0001. **d,** Western blot analysis of EGFR, AXL, MET, p-AKT, AKT, p-MEK, MEK, p-ERK, ERK, p-RSK, RSK, and GAPDH in exarafenib-resistant cell lines transfected with indicated siRNA and treated with 500 nM exarafenib for 4 hours. **e,** MAPK pathway analysis in NCI-H2405 parental and resistant cells treated with exarafenib (500 nM) for 4 hours under low (3%) or high (10%) FBS conditions.

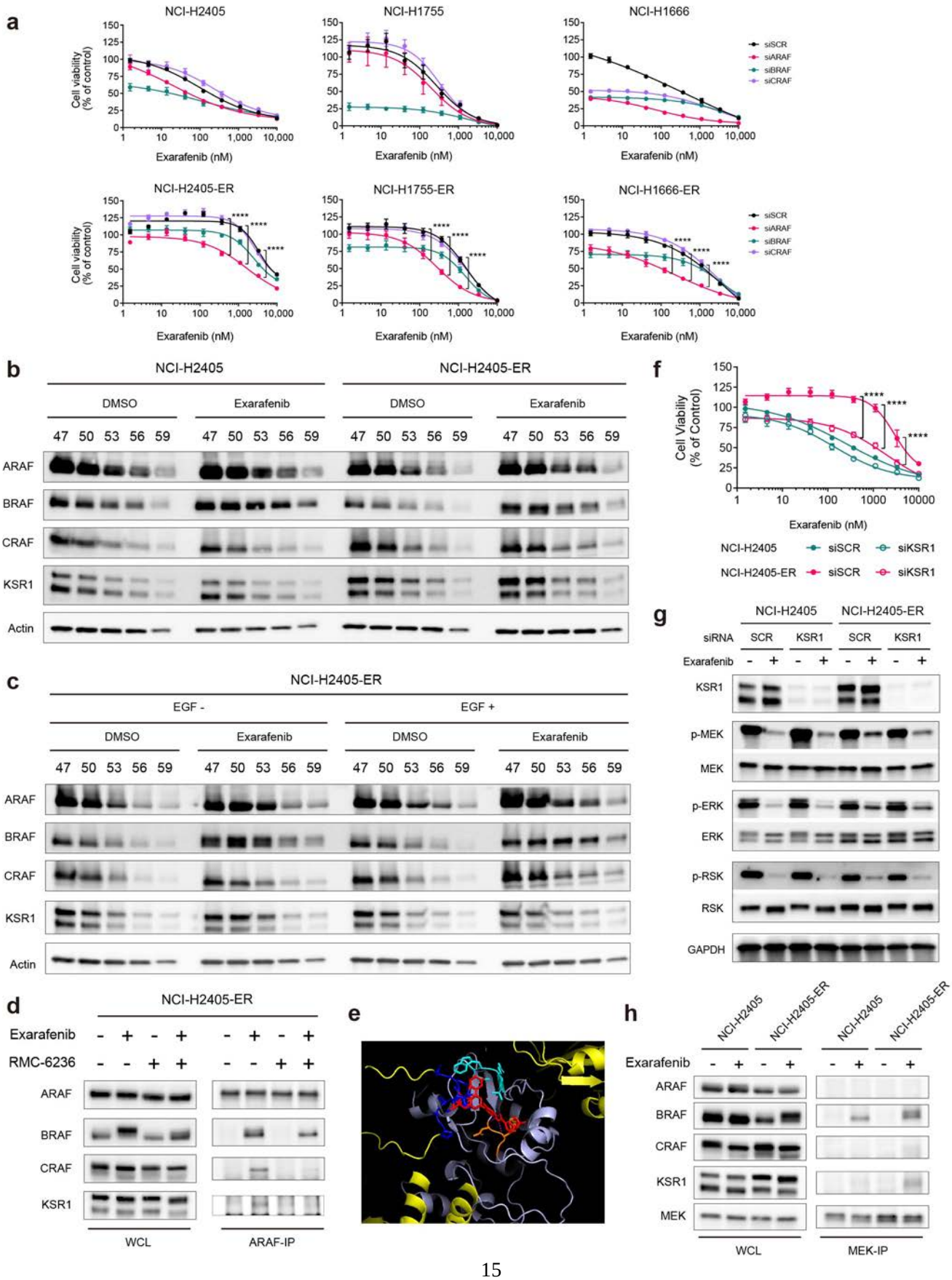
a
NCI-H2405
NCI-H1755
NCI-H1666
NCI-H2405-ER
NCI-H1755-ER
NCI-H1666-ER
Cell viability (% of control)
Exarafenib (nM)
siSCR
siARAF
siBRAF
siCRAF
b
NCI-H2405
NCI-H2405-ER
DMSO
Exarafenib
47 50 53 56 59
ARAF
BRAF
CRAF
KSR1
Actin
c
NCI-H2405-ER
EGF -
EGF +
d
NCI-H2405-ER
Exarafenib
RMC-6236
WCL
ARAF-IP
e
f
Cell Viability (% of Control)
NCI-H2405 siSCR siKSR1
NCI-H2405-ER siSCR siKSR1
g
siRNA
SCR
KSR1
p-MEK
MEK
p-ERK
ERK
p-RSK
RSK
GAPDH
h
MEK-IP

Supplementary Figure 8. Molecular characterization of ARAF-KSR1 complex-mediated resistance mechanism and functional validation of RAF isoform dependencies

a, Dose-response curves for RAF isoform knockdown experiments. Cell viability was measured in parental (top) and exarafenib-resistant (bottom) cell lines following transfection with scrambled control (siSCR, black), siARAF (red), siBRAF (green), or siCRAF (purple) and treatment with increasing concentrations of exarafenib. Data represent mean ± SD. ****P < 0.0001. Heatmap depicting the IC50 value is shown in Fig. 5a. **b,** CETSA analysis of RAF isoforms and KSR1 in parental and resistant cells treated with DMSO or exarafenib (500 nM) for 24 hours. Exarafenib enhanced thermal stabilization of ARAF and CRAF in resistant cells, while BRAF stabilization was largely maintained. KSR1 showed minimal stabilization. **c,** CETSA analysis of exarafenib-resistant NCI-H2405-ER cells treated with DMSO or exarafenib (500 nM) for 24 hours, with or without EGF stimulation. EGF enhanced exarafenib-induced thermal stabilization of all RAF isoforms. KSR1 showed minimal stabilization regardless of EGF. **d,** Co-immunoprecipitation analysis investigating RAS-dependent regulation of ARAF-KSR1 complex formation. NCI-H2405-ER cells were treated with DMSO, exarafenib (500 nM), RMC-6236 (1 μM), or combination of both for 24 hours. ARAF immunoprecipitation demonstrates that the multi-RAS inhibitor RMC-6236 suppresses ARAF-KSR1 interaction, confirming RAS-dependent regulation of this protein complex. **e,** Docking analysis of exarafenib in the AlphaFold-predicted ARAF–KSR1 complex. Exarafenib binds the ATP pocket of ARAF, contacting the hinge region and DFG motif, with additional contacts to a short KSR1 segment. ARAF chain: gray, KSR1 chain: yellow, Exarafenib: red, ARAF gatekeeper and hinge region (Thr382–Cys385): Cyan, ARAF DFG motif (Asp447–Phe448–Gly449): orange, KSR1 segment (Pro408–Asn413): blue, Chemical bonds: magenta. **f,** Cell viability dose-response curves showing the effect of KSR1 knockdown on exarafenib sensitivity in NCI-H2405 parental and resistant cells. Cells were transfected with scrambled control (SCR) or KSR1 siRNA (siKSR1) and treated with increasing concentrations of exarafenib. Data represent mean ± SD. ****P < 0.0001. Heatmap depicting the IC50 value is shown in Fig. 5h. **g,** Western blot analysis of MAPK pathway components in NCI-H2405 and NCI-H2405-ER cells following KSR1 knockdown and exarafenib treatment. Cells were transfected with scrambled control (SCR) or KSR1 siRNA and treated with exarafenib (+) or vehicle (-). **h,** Co-immunoprecipitation analysis of MEK complexes in parental (NCI-H2405) and resistant (NCI-H2405-ER) cells treated with DMSO or exarafenib (500 nM) for 24 hours.

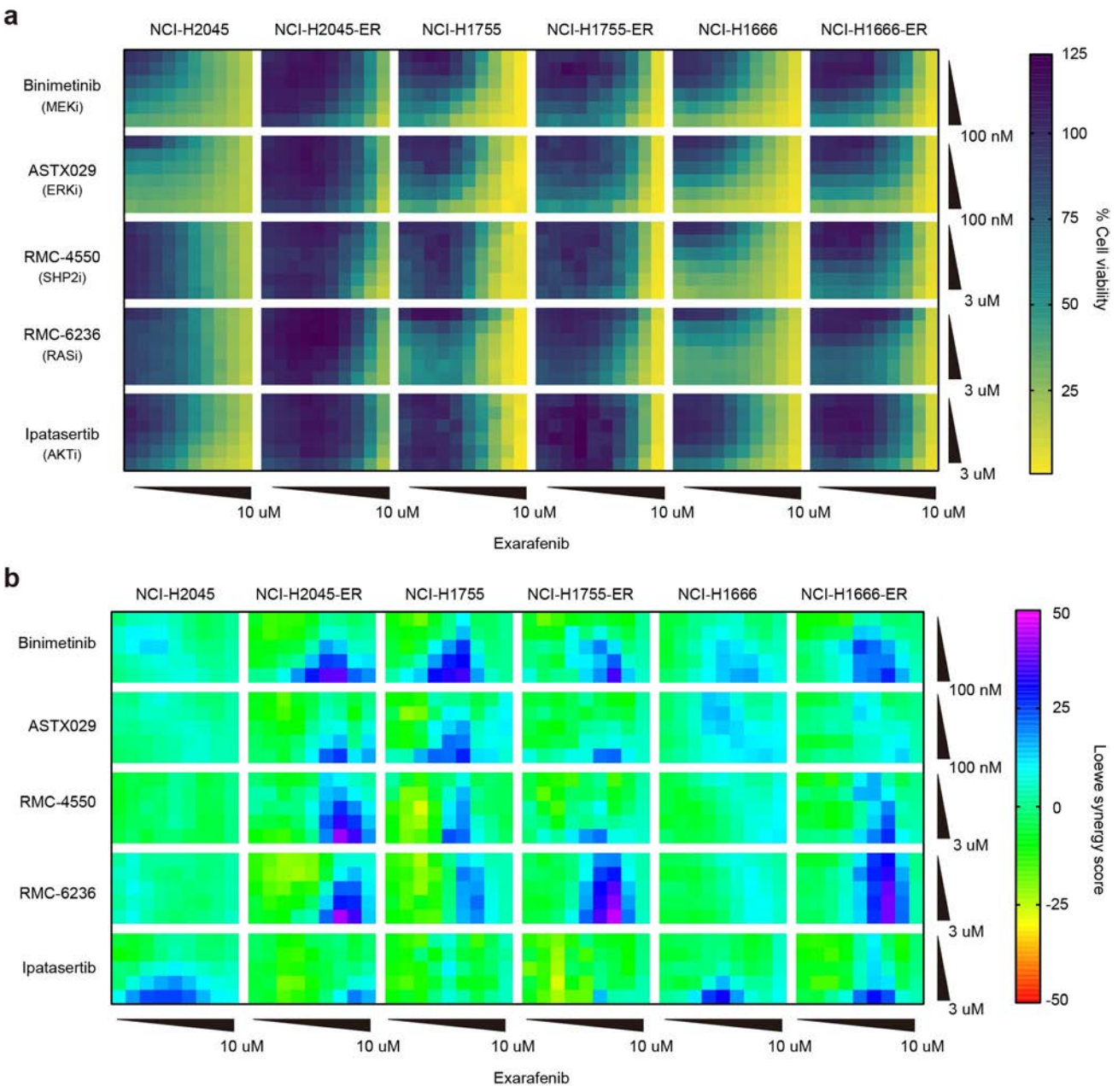

Supplementary Figure 9. Effects of exarafenib combined with binimetinib, ASTX029, RMC-4550, RMC-6236 and ipatasertib in parental and exarafenib-resistant lung cancer cell lines.

a, Heatmap of cell viability for exarafenib combined with binimetinib, ASTX029, RMC-4550, RMC-6236 or ipatasertib in parental and resistant NCI-H2405, NCI-H1755, and NCI-H1666 cells. Lighter shades represent more potent inhibition. **b,** Heatmap of synergy scores for exarafenib combined with binimetinib, ASTX029, RMC-4550, or ipatasertib in parental and exarafenib-resistant NCI-H2405, NCI-H1755, and NCI-H1666 cell lines. Synergy scores were calculated using the Loewe model on dataset from (**a**). Positive scores indicate synergy.

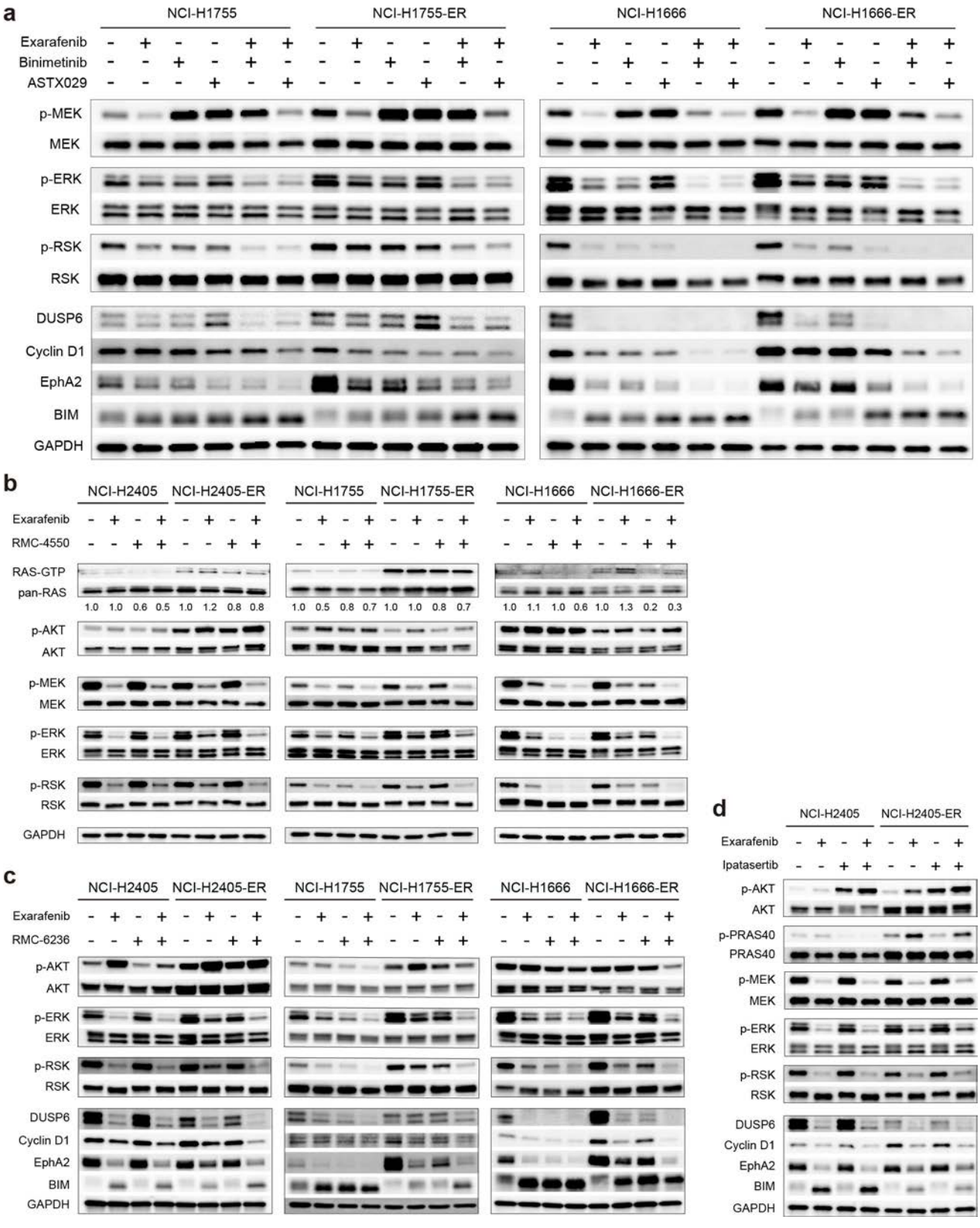
a
NCI-H1755
NCI-H1755-ER
NCI-H1666
NCI-H1666-ER
Exarafenib
Binimetinib
ASTX029
p-MEK
MEK
p-ERK
ERK
p-RSK
RSK
DUSP6
Cyclin D1
EphA2
BIM
GAPDH
b
NCI-H2405
NCI-H2405-ER
NCI-H1755
NCI-H1755-ER
NCI-H1666
NCI-H1666-ER
Exarafenib
RMC-4550
RAS-GTP
pan-RAS
1.0 1.0 0.6 0.5 1.0 1.2 0.8 0.8
1.0 0.5 0.8 0.7 1.0 1.0 0.8 0.7
1.0 1.1 1.0 0.6 1.0 1.3 0.2 0.3
p-AKT
AKT
p-MEK
MEK
p-ERK
ERK
p-RSK
RSK
GAPDH
c
NCI-H2405
NCI-H2405-ER
NCI-H1755
NCI-H1755-ER
NCI-H1666
NCI-H1666-ER
Exarafenib
RMC-6236
p-AKT
AKT
p-ERK
ERK
p-RSK
RSK
DUSP6
Cyclin D1
EphA2
BIM
GAPDH
d
NCI-H2405
NCI-H2405-ER
Exarafenib
Ipatasertib
p-AKT
AKT
p-PRAS40
PRAS40
p-MEK
MEK
p-ERK
ERK
p-RSK
RSK
DUSP6
Cyclin D1
EphA2
BIM
GAPDH

Supplementary Figure 10. Mechanistic insights and combinatorial efficacy of exarafenib and MAPK pathway inhibitors in lung cancer cell lines.

a, Immunoblot analysis of MEK, ERK, and RSK phosphorylation, along with DUSP6, Cyclin D1, EphA2, BIM, and GAPDH expression in parental and exarafenib-resistant NCI-H1755 and NCI-H1666 cell lines treated with exarafenib (500 nM), binimetinib (50 nM), ASTX029 (50 nM), or a combination of exarafenib with either binimetinib or ASTX029 for 48 hours. **b,** Analysis of RAS-GTP levels, total RAS, AKT activation, and key MAPK signaling components in parental and exarafenib-resistant NCI-H2405, NCI-H1755, and NCI-H1666 cell lines treated with exarafenib (500 nM), RMC-4550 (1 μM), or a combination of both for 4 hours. Drug concentrations were selected based on their high synergy scores in resistant cells, as calculated from the comprehensive drug screening (Supplementary Fig. 9b). **c,** Immunoblot analysis of p-AKT, AKT, p-MEK, MEK, p-ERK, ERK, p-RSK, RSK, DUSP6, Cyclin D1, EphA2, BIM, and GAPDH levels in parental and exarafenib-resistant NCI-H2405, NCI-H1755 and NCI-H1666 cell lines treated with exarafenib (500 nM), RMC-6236 (1 μM), or a combination of both for 48 hours. **d,** Examination of AKT and PRAS40 phosphorylation alongside MAPK signaling regulators, including DUSP6, Cyclin D1, EphA2, and BIM, in parental and exarafenib-resistant NCI-H2405 cells treated with exarafenib (500 nM), ipatasertib (1 μM), or a combination of both for 48 hours. The phosphorylation state of the PRAS40 protein, a downstream target of AKT, was included to verify the activity of ipatasertib.

a

IC50 (nM)	MEK inhibitor			ERK inhibitor		
	Binimetinib	Cobimetinib	Trametinib	ASTX029	SCH772984	LY3214996
NCI-H2405	76.1	25.9	0.2	4.9	35.2	235.1
NCI-H1755	115.1	27.7	1.0	75.1	232.6	1,372.0
NCI-H1666	47.0	23.8	1.0	16.9	184.5	664.4

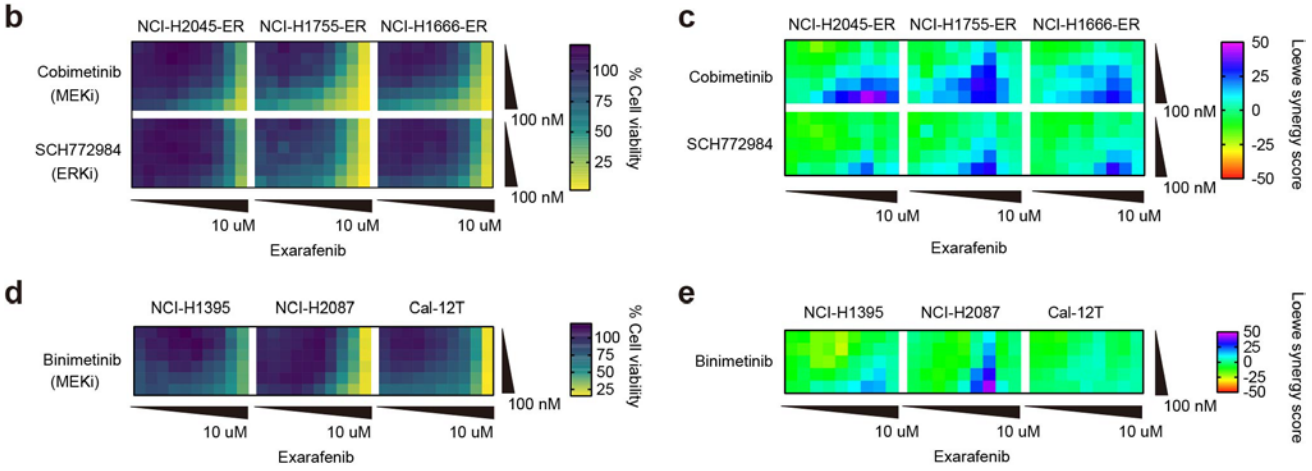

Supplementary Figure 11. Extended analysis of exarafenib's efficacy in combination with MAPK pathway blockade.

a, IC50 values for MEK inhibitors (binimetinib, cobimetinib, trametinib) and ERK inhibitors (ASTX029, SCH772984, LY3214996) in NCI-H2405, NCI-H1755, and NCI-H1666 cell lines calculated by cell viability assay. **b, d**, Cell viability heatmaps for exarafenib combined with cobimetinib or SCH772984 in NCI-H2045-ER, NCI-H1755-ER, and NCI-H1666-ER cells (**b**), and exarafenib combined with binimetinib in NCI-H1395, NCI-H2087, and Cal-12T cells (**d**). Heatmaps represent the percentage of viable cells relative to untreated control. **c, e**, Synergy scores for exarafenib combinations in panels (**b**) and (**d**), respectively, calculated using the Loewe model. Positive scores indicate synergy.

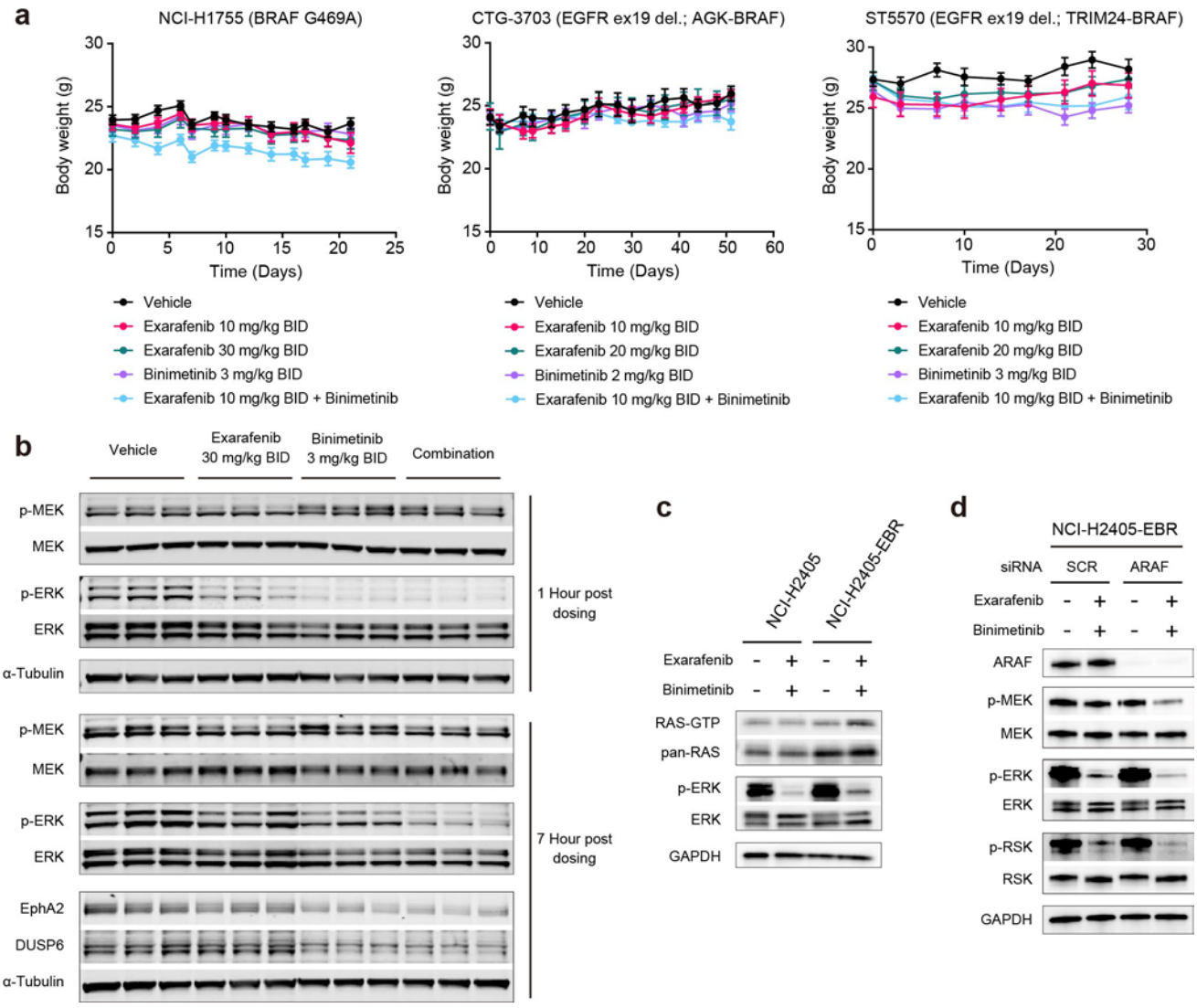

Supplementary Figure 12. *In vivo* tolerability and pharmacodynamic effects of exarafenib plus binimetinib combination therapy, and ARAF-mediated resistance mechanisms.

a, Body weight curves for xenograft mouse models treated with vehicle, exarafenib (10, 20, or 30 mg/kg, BID), binimetinib (2 or 3 mg/kg, BID), or their combination. Models: NCI-H1755 (BRAF G469A), CTG-3703 (AGK-BRAF), and ST5570 (TRIM24-BRAF). Data: mean ± s.e.m. (n = 9 for NCI-H1755; n = 6 for CTG-3703 and ST5570). **b,** Western blot analysis of H1755 xenograft tumor samples at 1-hour and 7-hours post-dosing with vehicle, exarafenib (30 mg/kg BID), binimetinib (3 mg/kg BID), and their combination. Three independent samples from each group were analyzed. Levels of p-MEK, MEK, p-ERK, ERK, EphA2, DUSP6, and α-Tubulin were assessed. **c,** RAS-GTP pulldown assays in NCI-H2405 parental and combination-resistant (EBR) cells. Cells were treated with exarafenib (500 nM) in combination with binimetinib (50 nM) for 24 hours. EBR cells exhibit elevated RAS-GTP levels under combination drug treatment compared to parental cells. **d,** Western blot analysis of MAPK pathway

components in NCI-H2405-EBR cells following ARAF knockdown. Cells were transfected with scrambled control (SCR) or ARAF siRNA and treated with exarafenib (500 nM) and binimetinib (50 nM) combination for 24 hours.

2. Supplementary Tables

Supplementary Table 1. Clinical Characteristics

Parameter		BRAF Class			Pairwise Chi-squared test with Holm adj.*P*-value		
		Class I	Class II	Class III	I vs II	I vs III	II vs III
	N	845	810	743			
Age							
	Mean	68.61	70.1	69.37			
	Std Deviation	11.01	9.7	10.47			
	Median	70	70	70			
	Min	23	42	41			
	Max	85	85	85			
Gender					*	*	ns
Female	Frequency	476	410	371	0.0451	0.0373	0.827
	Percent (%)	56.33	50.62	49.93			
Male	Frequency	369	400	372			
	Percent (%)	43.67	49.38	50.07			
Tobacco Use					****	****	ns
Ever Tobacco Product User	Frequency	462	559	509	8.18×10^{-9}	4.52×10^{-8}	0.873
	Percent (%)	54.67	69.01	68.51			
Unknown	Frequency	383	251	234			
	Percent (%)	45.33	30.99	31.49			

Patients with multiple BRAF alterations across functional classes were excluded from the summary of characteristics. Pairwise Chi-squared test with holm *P*-value adjustment was used to compare frequencies across BRAF Classes. *$P < 0.05$, **$P < 0.01$, ***$P < 0.001$, ****$P < 0.0001$.

Supplementary Table 2. Residues contacting exarafenib in the AlphaFold-predicted ARAF–KSR1 complex

Chain	Residue name	Residue number	Min Distance (Å)
ARAF	VAL	324	3.86
ARAF	ALA	334	2.6
ARAF	VAL	335	3.4
ARAF	LYS	336	2.57
ARAF	GLU	354	2.99
ARAF	VAL	357	3.6
ARAF	LEU	358	2.2
ARAF	THR	361	2.37
ARAF	ILE	366	3.11
ARAF	LEU	367	3.68
ARAF	ILE	380	2.94
ARAF	ILE	381	4.77
ARAF	THR	382	2.75
ARAF	GLN	383	1.62
ARAF	TRP	384	2.19
ARAF	CYS	385	2.14
ARAF	LEU	420	2.72
ARAF	ILE	425	4.47
ARAF	PHE	436	2.62
ARAF	ILE	445	4.41
ARAF	GLY	446	4.12
ARAF	ASP	447	3.41
ARAF	PHE	448	0.7
ARAF	GLY	449	3.57
ARAF	ALA	451	4.23
KSR1	PRO	408	4.21
KSR1	SER	409	1.6
KSR1	ASP	410	2.46
KSR1	ILE	411	0.67
KSR1	ASN	412	1.88
KSR1	ASN	413	4.79

Supplementary Table 3. Antibody List

Protein		Site	Product No.	Manufacturer	Species
pan-RAS	total		AESA02	Cytoskeleton	Mouse
ARAF	total		sc-166771	Santa Cruz	Mouse
	total		sc-408	Santa Cruz	Rabbit
BRAF	total		sc-5284	Santa Cruz	Mouse
	total		14814	Cell Signaling Technology	Rabbit
CRAF	total		BD-610152	BD Biosciences	Mouse
	total		9422	Cell Signaling Technology	Rabbit
KSR1	total		MA5-53956	Invitrogen	Rabbit
MEK	phospho	Ser217/221	9154	Cell Signaling Technology	Rabbit
	phospho	Ser218/222	sc-81503	Santa Cruz	Mouse
	total		BD-610122	BD Biosciences	Mouse
	total		CST 9122	Cell Signaling Technology	Rabbit
ERK	phospho	Thr202/Tyr204	9101	Cell Signaling Technology	Rabbit
	total		9102	Cell Signaling Technology	Rabbit
RSK	phospho	Thr359/Ser363	9344	Cell Signaling Technology	Rabbit
	total		9355	Cell Signaling Technology	Rabbit
AKT	phospho	Ser473	4060	Cell Signaling Technology	Rabbit
	total		4691	Cell Signaling Technology	Rabbit
PRAS40	phospho	Thr246	13175	Cell Signaling Technology	Rabbit
	total		2610	Cell Signaling Technology	Rabbit
DUSP6	total		39441	Cell Signaling Technology	Rabbit
Cyclin D1	total		55506	Cell Signaling Technology	Rabbit
EphA2	total		6997	Cell Signaling Technology	Rabbit
BIM	total		2933	Cell Signaling Technology	Rabbit
EGFR	total		4267	Cell Signaling Technology	Rabbit
AXL	total		8661	Cell Signaling Technology	Rabbit
MET	total		8198	Cell Signaling Technology	Rabbit
GAPDH	total		sc-365062	Santa Cruz	Mouse
CHK2	phospho	Thr68	2661	Cell Signaling Technology	Rabbit
H2A.X	phospho	Ser139	2577	Cell Signaling Technology	Rabbit
PARP	total		9542	Cell Signaling Technology	Rabbit